IET Communications

Research Article

IET Journals
The Institution of Engineering and Technology

Modelling, analysis and performance comparison of two direct sampling DCSK receivers under frequency non-selective fading channels

ISSN 1751-8628
Received on 22nd November 2015
Revised on 1st March 2016
Accepted on 28th March 2016
doi: 10.1049/iet-com.2015.1103
www.ietdl.org

Nguyen Xuan Quyen[1] ✉, *Trung Q. Duong*[2,3], *Arumugam Nallanathan*[4]

[1]*Hanoi University of Science and Technology, Hanoi, Vietnam*
[2]*Queen's University Belfast, Belfast, UK*
[3]*Duy Tan University, Vietnam*
[4]*King's College London, London, UK*
✉ *E-mail: quyen.nguyenxuan@hust.edu.vn*

Abstract: Two direct sampling correlator-type receivers for differential chaos shift keying (DCSK) communication systems under frequency non-selective fading channels are proposed. These receivers operate based on the same hardware platform with different architectures. In the first scheme, namely sum-delay-sum (SDS) receiver, the sum of all samples in a chip period is correlated with its delayed version. The correlation value obtained in each bit period is then compared with a fixed threshold to decide the binary value of recovered bit at the output. On the other hand, the second scheme, namely delay-sum-sum (DSS) receiver, calculates the correlation value of all samples with its delayed version in a chip period. The sum of correlation values in each bit period is then compared with the threshold to recover the data. The conventional DCSK transmitter, frequency non-selective Rayleigh fading channel, and two proposed receivers are mathematically modelled in discrete-time domain. The authors evaluated the bit error rate performance of the receivers by means of both theoretical analysis and numerical simulation. The performance comparison shows that the two proposed receivers can perform well under the studied channel, where the performances get better when the number of paths increases and the DSS receiver outperforms the SDS one.

1 Introduction

Wireless networks can be divided into two main categories, i.e. wireless local area networks (WLANs) and wireless personal area networks (WPANs) [1], where the former is designed for applications with high data rate and relatively long distance [2]. Most modern WLANs are based on IEEE 802.11 standards, marketed under the WiFi brand name [3]. In contrast, the latter mainly focus on low data rate and short distance applications [2]. It is known that communication technologies today are robustly developing in the direction of increasingly enhancing data rate over a given frequency band. Nevertheless, this does not mean that the low data rate applications are less important. In fact, low data applications are more popular and closer to our daily lives, such as: industrial control and monitoring; environmental and health monitoring; home automation, entertainment and toys; security, location and asset tracking; emergency and disaster response [4]. Bluetooth technique with IEEE 802.15.1 standard is the first standard targeting at low data rate applications [5]. However, the complexity of this technique makes it unsuitable for simple applications requiring low cost and low power consumption. Owing to this reason, IEEE released a new standard for low rate WPANs (LR-WPANs), i.e. IEEE 802.15.4, which was intended to be simpler and less expensive than Bluetooth. A typical example of LR-WPANs with this standard is wireless sensor networks using Zigbee [6], which have been used widely in practical applications so far.

This work is inspired by the research gap as to how to design secure physical layer for LR-WPANs with the use of chaos-based communication schemes [7–9]. Among all the schemes proposed so far, chaos-based direct sequence/code division multiple access (DS/CDMA) [10–16] and different chaos shift keying (DCSK) [17, 18] have been studied widely. Compared with the chaos-based DS/CDMA schemes, the DCSK schemes with non-coherent receivers do not need chaotic sequence synchronisation, nor channel estimation, but only require symbol rate sampling [19]. Owing to the simple structure, the DCSK schemes are promising and feasible for hardware implementations [20, 21]. Particularly, the performance of the conventional DCSK scheme over additive white Gaussian noise (AWGN) channel and multipath fading channel was investigated in [22–24] and then extended to multipath fading channel with delay spread in [25–27]. The work in [28] presented a study on ultra-wideband direct chaotic communication technology using the DCSK scheme for LR-WPANs applications, however the system performance was only evaluated by numerical simulations. Beside the conventional scheme, multiple extended DCSK schemes have been proposed, such as frequency-modulated DCSK [29], permutation-based DCSK [30], reference-modulated DCSK [31], high-data-rate DCSK [32], high-efficiency DCSK [33], multi-carrier DCSK [34], DCSK-automatic repeat request/cooperative automatic repeat request (ARQ/CARQ) [35], improved DCSK [36] and so on, which aim at improving the system properties, e.g. data rate, spectrum efficiency, bit error rate (BER) performance, and physical layer security under different transmission environments. In particular, several works have recently been conducted focusing on improving the performance of DCSK communication schemes over wireless environments. The combined schemes of DCSK and diversity techniques, such as single-input multiple-output (SIMO) FM-DCSK [37], multiple-input multiple-output (MIMO) M-DCSK [38], MIMO-Relay DCSK-CD [39], and cooperative communication DCSK [40], were proposed as robust solutions to achieve this improvement. However, for the applications in LR-WPANs, the extended and diversity-combined DCSK schemes are impractical due to their complexity, which leads to high cost, high size, and high power consumption of the nodes in the networks.

In this paper, we propose a novel idea of applying oversampling technique [41] to the conventional DCSK receiver. The main

motivation for this study is expressed by both application and academic aspects as follows: (1) the design problem of a low-complexity and easy-implementation DCSK receiver, which can exploit the non-selective fading characteristic of low data-rate multipath channels in order to obtain a good performance for applications in LR-WPANs; (2) most previous studies on the performance of DCSK systems over multipath fading channels have been carried out under the context of high data-rate transmission [25, 34, 37, 39]. In this study, we propose and fully investigate DCSK receiver schemes over low data-rate multipath fading channel in terms of mathematical models, theoretical performance analysis, and numerical simulations. These obtained models and analysis could motivate the next studies on chaos-based low-rate wireless communications. At the input of the receiver, the received signal is directly sampled at a sampling rate higher than chip rate. This direct sampling is to help the receiver specifically determine delayed-signal components of the received signal from fading multipath channels, which can be combined together by a correlation process in order to increase the ratio of signal-to-noise at the output. The improvement of communication features at receiving side by means of the oversampling technique has been studied in [42, 43]. There are two possible different architectures for the receiver, i.e. Sum-Delay-Sum (SDS) and Delay-Sum-Sum (DSS), which are designed for operating on the same optimal hardware platform. In the SDS receiver, the sum of all samples in each chip period is correlated with its delayed version. The correlation value obtained in each bit period is then compared with a fixed threshold to decide binary value of the recovered bit. On the other hand, the DSS receiver calculates the correlation value of the samples with its delayed version in each chip duration. The sum of all correlation values in each bit period is compared with the threshold to recover the data. Since any two nodes in LR-WPANs communicate to each other in short distance at low rate, the root-mean-square delay spread is less than the chip period, the wireless transmission environment between them can be considered as a frequency non-selective fading channel [44]. Therefore, the operation and performance of two proposed receivers at the physical layer of LR-WPANs are modelled and analysed in the scenario of whole communication system, including the conventional DCSK transmitter and frequency non-selective Rayleigh fading channel. The performance comparison will show us which receiver outperforms the other. The better one along with the conventional transmitter is a simple and effective solution for the design of secure physical layer in LR-WPANs.

The rest of this paper is organised as follows. Section 2 presents the mathematical models in the discrete-time domain for the conventional DCSK transmitter, frequency non-selective Rayleigh fading channel, and two proposed receivers. The BER performance of the receivers is analysed by means of theoretical derivation and numerical computation in Section 3. In Section 4, simulation results are shown to verify the analysis ones, simultaneously the performances of two receivers are compared with each other. The implementation complexity of the proposed receivers is discussed in Section 5 and our conclusion is given in Section 6.

2 Mathematical modelling in discrete-time domain

Fig. 1*a* shows block diagrams of the conventional transmitter and the frequency non-selective Rayleigh fading channel. Block diagrams of the SDS and DSS receivers are displayed in Figs. 1*b* and *c*, respectively.

2.1 Modelling of transmitter and L-path channel

In the DCSK transmitter, each data bit period, denoted by T_b, consists of two bit halves with equal duration $T_b/2$. The chip

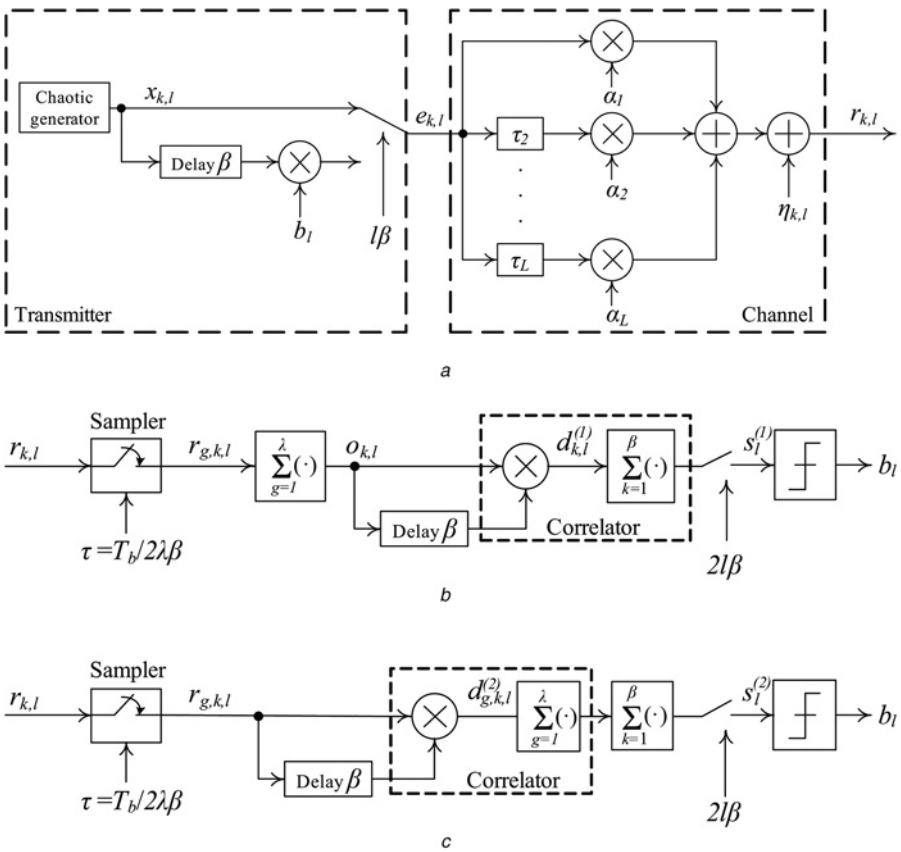

Fig. 1 *Block diagram of the DCSK communication system under study*

a Conventional transmitter and the frequency non-selective Rayleigh fading channel with *L*-path
b Sum-delay-sum receiver and
c Delay-sum-sum Receiver

IET Commun., 2016, Vol. 10, Iss. 11, pp. 1263–1272

period of the chaotic sequence is T_c. The ratio, $2\beta = T_b/T_c$, i.e. number of chips per bit, is called as the spreading factor of the system. The first half is used to transmit the chaotic reference sequence. The second half is to transmit the data-bearing sequence which is a copy of the reference sequence if '+1' bit is sent or an inverted copy of the reference sequence if '−1' bit is sent. The transmitted signal for the lth data bit is given by

$$e_{k,l} = \begin{cases} x_{k,l}, & k = 1, \ldots, \beta, \\ b_l x_{k-\beta,l}, & k = \beta + 1, \ldots, 2\beta, \end{cases} \quad (1)$$

where $b_l = \pm 1$ is binary value of the lth bit, $x_{k,l}$ is value of the kth chip in the lth bit in the reference sequence and $x_{k-\beta,l}$ is the delayed version of $x_{k,l}$.

The frequency non-selective fading channel model is assumed to have L paths, where the path having the shortest transmission period is considered as the primary path with delay being zero and all others are the secondary paths with non-zero delays. The system performance is investigated under the condition that the transmitter and receiver are stationary, thus phase variations of the received signals in primary and secondary channels can be ignored. The impulse response of the channel can be written as

$$h(n) = \sum_{j=1}^{L} \alpha_j \delta\left(n - \tau_j\right), \quad (2)$$

where $\delta(t)$ is the Dirac impulse; τ_j and α_j is the time delay and fading coefficient of the jth path, respectively. The 1st path is the primary path having $\alpha_1 > 0$ and $\tau_1 = 0$. The jth paths with $j = 2, 3, \ldots, L$ are the secondary paths with $\alpha_j > 0$ and $\tau_j > 0$. Because of the non-selective fading characteristic, without of generality, the chip period and channel delays are assumed to be equal to a multiple of the sampling cycle τ, i.e. the time period between two consecutive samples in the receiver and simultaneously satisfies the following conditions, $\tau_1 = 0 \le \tau_2 \le \tau_3 \le \cdots \le \tau_L \le T_c$. For the sake of mathematical representation, we denote $\lambda = T_c/\tau$, $\lambda_j = \tau_j/\tau$ and $\tau_{L+1} = T_c$, thus $\lambda_{L+1} = \lambda$. It means that there are λ samples in a chip period T_c and λ_j samples in each corresponding delay τ_j. The fading coefficients α_j vary randomly according to the Rayleigh distribution given by

$$f(\alpha_j) = \frac{\alpha_j}{\sigma_j^2} e^{-\alpha_j^2/(2\sigma_j^2)}, \quad (3)$$

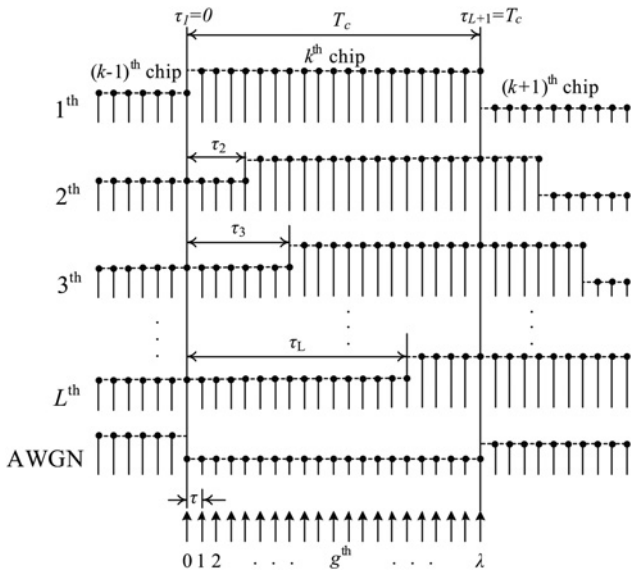

Fig. 2 *Illustration of the multipath components of the received signal and the sampling process in the receivers*

with σ_j, the scale parameter of the distribution, being constant. The mean and mean squared values of each fading coefficient are, respectively, determined by $E[\alpha_j] = \sigma_j\sqrt{\pi/2}$ and $E[\alpha_j^2] = 2\sigma_j^2$. Under the above assumptions, the output signal of the channel can be expressed by the following sum

$$r_{k,l} = \alpha_1 e_{k,l} + \alpha_2 e_{k-\tau_2,l} + \cdots + \alpha_L e_{k-\tau_L,l} + \eta_{k,l}. \quad (4)$$

where $\eta_{k,\,l}$ is the AWGN with a zero mean value.

2.2 Modelling of sum-delay-sum receiver

The received signal $r_{k,\,l}$ is fed to the sampler operating at a sampling rate, $SR = 1/\tau = 2\beta\lambda/T_b = \lambda/T_c$, where λ is the number of samples per chip. Fig. 2 illustrates components of the signal $r_{k,\,l}$ and their sampling process in the SDS and DSS receivers within the period of kth chip in the second half of lth bit. It can be seen that in the considered period, the received signal consists of three components, i.e. the kth chip and its delayed parts within the period of $(T_c - \tau_j)$, the delayed parts within the period τ_j of the $(k-1)$th chip, and AWGN. We find that there are $(\lambda_{j+1} - \lambda_j)$ samples in the duration of $(\tau_j, \tau_{j+1}]$, all of which have the same value which is determined by

$$\begin{aligned} r_{g,k,l} &= \alpha_1 e_{k,l} + \cdots + \alpha_j e_{k,l} + \alpha_{j+1} e_{k-1,l} + \cdots + \alpha_L e_{k-1,l} + \eta_{k,l} \\ &= e_{k,l} \sum_{i=1}^{j} \alpha_i + e_{k-1,l} \sum_{i=j+1}^{L} \alpha_i + \eta_{k,l}, \\ &= b_l x_{k-\beta,l} \sum_{i=1}^{j} \alpha_i + b_l x_{(k-1)-\beta,l} \sum_{i=j+1}^{L} \alpha_i + \eta_{k,l}, \end{aligned} \quad (5)$$

where $r_{g,\,k,\,l}$ is the value of the gth sample in the kth chip duration, satisfying $\lambda_j < g \le \lambda_{j+1}$. The sample $r_{g,\,k,\,l}$ is fed to a sum block, in which the consecutive samples at input are added together in each chip duration to produce the signal $o_{k,\,l}$ given by

$$\begin{aligned} o_{k,l} &= \sum_{g=1}^{\lambda} r_{g,k,l} = b_l x_{k-\beta,l} \sum_{j=1}^{L} (\lambda_{j+1} - \lambda_j) \sum_{i=1}^{j} \alpha_i + b_l x_{(k-1)-\beta,l} \\ &\quad \sum_{j=1}^{L} (\lambda_{j+1} - \lambda_j) \sum_{i=j+1}^{L} \alpha_i + \lambda \eta_{k,l}. \end{aligned} \quad (6)$$

The signal $o_{k,l}$ is then correlated to it delayed version $o_{k-\beta,\,l}$. The resulting correlation values are summed over the second half of each bit period to produce the decision variable $s_l^{(1)}$ expressed by

$$\begin{aligned} s_l^{(1)} &= \sum_{k=1}^{\beta} d_{k,l}^{(1)} = \sum_{k=1}^{\beta} o_{k,l} o_{k-\beta,l} \\ &= A^2 b_l \sum_{k=1}^{\beta} x_{k-\beta,l}^2 + B^2 b_l \sum_{k=1}^{\beta} x_{(k-1)-\beta,l}^2 \\ &\quad + 2AB b_l \sum_{k=1}^{\beta} x_{k-\beta,l} x_{(k-1)-\beta,l} \\ &\quad + \lambda \sum_{k=1}^{\beta} \left(A x_{k-\beta,l} + B x_{(k-1)-\beta,l}\right)\left(\eta_{k,l} + b_l \eta_{k-\beta,l}\right) \\ &\quad + \lambda^2 \sum_{k=1}^{\beta} \eta_{k,l} \eta_{k-\beta,l}, \end{aligned} \quad (7)$$

where

$$A = \sum_{j=1}^{L} (\lambda_{j+1} - \lambda_j) \sum_{i=1}^{j} \alpha_i, \tag{8}$$

$$B = \sum_{j=1}^{L} (\lambda_{j+1} - \lambda_j) \sum_{i=j+1}^{L} \alpha_i. \tag{9}$$

On the basis of value of the decision variable $s_l^{(1)}$, the binary value of the lth bit is finally recovered by the decision circuit using a sign function as follows

$$b_l = \begin{cases} 1 & s_l^{(1)} \geq 0, \\ -1 & s_l^{(1)} < 0. \end{cases} \tag{10}$$

2.3 Modelling of delay-sum-sum receiver

The sampling process of the received signal at the input of DSS receiver is totally similar as that in the above SDS receiver. Based on (5), we can, respectively, represent the value of samples in duration of $(\tau_j, \tau_{j+1}]$, i.e. $r_{g,k,l}$ and the signal at the output of the delay β block, i.e. $r_{g,k-\beta,l}$, as follows

$$r_{g,k,l} = b_l x_{k-\beta,l} \sum_{i=1}^{j} \alpha_i + b_l x_{(k-1)-\beta,l} \sum_{i=j+1}^{L} \alpha_i + \eta_{k,l}, \tag{11}$$

and

$$r_{g,k-\beta,l} = x_{k-\beta,l} \sum_{i=1}^{j} \alpha_i + x_{(k-1)-\beta,l} \sum_{i=j+1}^{L} \alpha_i + \eta_{k-\beta,l}. \tag{12}$$

The value of samples in $(\tau_j, \tau_{j+1}]$ at the output of the multiplier is determined by

$$\begin{aligned} d_{g,k,l}^{(2)} &= r_{g,k,l} r_{g,k-\beta,l} \\ &= \left(\sum_{i=1}^{j} \alpha_i \right)^2 b_l x_{k-\beta,l}^2 + \left(\sum_{i=j+1}^{L} \alpha_i \right)^2 b_l x_{(k-1)-\beta,l}^2 \\ &\quad + 2 \sum_{i=1}^{j} \alpha_i \sum_{i=j+1}^{L} \alpha_i b_l x_{k-\beta,l} x_{(k-1)-\beta,l} \\ &\quad + \left(\sum_{i=1}^{j} \alpha_i x_{k-\beta,l} + \sum_{i=j+1}^{L} \alpha_i x_{(k-1)-\beta,l} \right) \\ &\quad \left(\eta_{k,l} + b_l \eta_{k-\beta,l} \right) + \eta_{k,l} \eta_{k-\beta,l}. \end{aligned} \tag{13}$$

In the sum block, the consecutive samples at input are added together in each second half of bit period to produce a decision variable $s_l^{(2)}$ as

$$\begin{aligned} s_l^{(2)} &= \sum_{k=1}^{\beta} \sum_{g=1}^{\lambda} d_{g,k,l}^{(2)} = \sum_{k=1}^{\beta} \sum_{j=0}^{L} (\lambda_{j+1} - \lambda_j) d_{g,k,l}^{(2)} \\ &= C b_l \sum_{k=1}^{\beta} x_{k-\beta,l}^2 + D b_l \sum_{k=1}^{\beta} x_{(k-1)-\beta,l}^2 + 2E b_l \sum_{k=1}^{\beta} x_{k-\beta,l} x_{(k-1)-\beta,l} \\ &\quad + A \sum_{k=1}^{\beta} x_{k-\beta,l} \left(\eta_{k,l} + b_l \eta_{k-\beta,l} \right) \\ &\quad + B \sum_{k=1}^{\beta} x_{(k-1)-\beta,l} \left(\eta_{k,l} + b_l \eta_{k-\beta,l} \right) + \lambda \sum_{k=1}^{\beta} \eta_{k,l} \eta_{k-\beta,l}, \end{aligned} \tag{14}$$

where

$$C = \sum_{j=1}^{L} (\lambda_{j+1} - \lambda_j) \left(\sum_{i=1}^{j} \alpha_i \right)^2, \tag{15}$$

$$D = \sum_{j=1}^{L} (\lambda_{j+1} - \lambda_j) \left(\sum_{i=j+1}^{L} \alpha_i \right)^2, \tag{16}$$

$$E = \sum_{j=1}^{L} (\lambda_{j+1} - \lambda_j) \sum_{i=1}^{j} \alpha_i \sum_{i=j+1}^{L} \alpha_i, \tag{17}$$

Finally, the binary value of the lth bit is recovered according to (10).

3 Performance analysis

This section presents the analysis of BER performance for two proposed DCSK receivers. The analysis process is carried out in two steps, i.e. theoretical derivation and numerical integration. For the sake of explanation, we classify and denote the signal components in the decision variables, i.e. $s_l^{(1)}$ and $s_l^{(2)}$, respectively, as follows

$$W_1 = A^2 b_l \sum_{k=1}^{\beta} x_{k-\beta,l}^2 + B^2 b_l \sum_{k=1}^{\beta} x_{(k-1)-\beta,l}^2, \tag{18}$$

$$X_1 = 2AB b_l \sum_{k=1}^{\beta} x_{k-\beta,l} x_{(k-1)-\beta,l}, \tag{19}$$

$$Y_1 = \lambda \sum_{k=1}^{\beta} \left(A x_{k-\beta,l} + B x_{(k-1)-\beta,l} \right) \left(\eta_{k,l} + b_l \eta_{k-\beta,l} \right), \tag{20}$$

$$Z_1 = \lambda^2 \sum_{k=1}^{\beta} \eta_{k,l} \eta_{k-\beta,l}, \tag{21}$$

and

$$W_2 = A b_l \sum_{k=1}^{\beta} x_{k-\beta,l}^2 + B b_l \sum_{k=1}^{\beta} x_{(k-1)-\beta,l}^2, \tag{22}$$

$$X_2 = C b_l \sum_{k=1}^{\beta} x_{k-\beta,l} x_{(k-1)-\beta,l}, \tag{23}$$

$$\begin{aligned} Y_2 &= D \sum_{k=1}^{\beta} x_{k-\beta,l} \left(\eta_{k,l} + b_l \eta_{k-\beta,l} \right) \\ &\quad + E \sum_{k=1}^{\beta} x_{(k-1)-\beta,l} \left(\eta_{k,l} + b_l \eta_{k-\beta,l} \right), \end{aligned} \tag{24}$$

$$Z_2 = \lambda \sum_{k=1}^{\beta} \eta_{k,l} \eta_{k-\beta,l}. \tag{25}$$

In the above equations, the components, i.e. W_1, X_1, Y_1, Z_1 of the variable $s_l^{(1)}$, and W_2, X_2, Y_2, Z_2 of the variable $s_l^{(2)}$, are random functions. Owing to the independence between fading coefficients and delays in the primary and secondary paths and their independence to AWGN, these components are also independent.

3.1 Theoretical derivation

First, the statistics of the components, i.e. W_1, X_1, Y_1, Z_1 and W_2, X_2, Y_2, Z_2, in the case of a '+1' bit transmitted are determined. Under the assumption that the value of β is high enough so that the correlation values of the independent variables in these components are

IET Commun., 2016, Vol. 10, Iss. 11, pp. 1263–1272

approximately equal to zero, the mean and mean squared values are determined as follows

$$E[W_1|b_l=+1]=(A^2+B^2)\beta E_c, \tag{26}$$

$$E[X_1|b_l=+1]=E[Y_1|b_l=+1]=E[Z_1|b_l=+1]=0. \tag{27}$$

$$E[W_1^2|b_l=+1]=(A^4+B^4)\beta(E_{c4}+(\beta-1)E_c^2)+2A^2B^2\beta^2E_c^2, \tag{28}$$

$$E[X_1^2|b_l=+1]=4A^2B^2\beta E_c^2, \tag{29}$$

$$E[Y_1^2|b_l=+1]=\lambda^2(A^2+B^2)\beta N_0E_c, \tag{30}$$

$$E[Z_1^2|b_l=+1]=\lambda^4\beta\frac{N_0^2}{4}, \tag{31}$$

with $E_c=E[x_{k,l}^2]$, $E_{c4}=E[x_{k,l}^4]$, $N_0=2E[\eta_{k,l}^2]$, and

$$E[W_2|b_l=+1]=(C+D)\beta E_c, \tag{32}$$

$$E[X_2|b_l=+1]=E[Y_2|b_l=+1]=E[Z_2|b_l=+1]=0. \tag{33}$$

$$E[W_2^2|b_l=+1]=(C^2+D^2)\beta(E_{c4}+(\beta-1)E_c^2)+2CD\beta^2E_c^2, \tag{34}$$

$$E[X_2^2|b_l=+1]=4E^2\beta E_c^2, \tag{35}$$

$$E[Y_2^2|b_l=+1]=(A^2+B^2)\beta N_0E_c, \tag{36}$$

$$E[Z_2^2|b_l=+1]=\lambda^2\beta\frac{N_0^2}{4}. \tag{37}$$

On the basis of the resulting values above, the variances of the components are calculated by

$$\begin{aligned}\mathrm{Var}[W_1|b_l=+1]&=E[W_1^2|b_l=+1]-E^2[W_1|b_l=+1]\\&=(A^4+B^4)\beta(E_{c4}-E_c^2),\end{aligned} \tag{38}$$

$$\begin{aligned}\mathrm{Var}[X_1|b_l=+1]&=E[X_1^2|b_l=+1]-E^2[X_1|b_l=+1]\\&=4A^2B^2\beta E_c^2,\end{aligned} \tag{39}$$

$$\begin{aligned}\mathrm{Var}[Y_1|b_l=+1]&=E[Y_1^2|b_l=+1]-E^2[Y_1|b_l=+1]\\&=\lambda^2(A^2+B^2))\beta N_0E_c,\end{aligned} \tag{40}$$

$$\begin{aligned}\mathrm{Var}[Z_1|b_l=+1]&=E[Z_1^2|b_l=+1]-E^2[Z_1|b_l=+1]\\&=\lambda^4\beta\frac{N_0^2}{4},\end{aligned} \tag{41}$$

and

$$\begin{aligned}\mathrm{Var}[W_2|b_l=+1]&=E[W_2^2|b_l=+1]-E^2[W_2|b_l=+1]\\&=(C^2+D^2)\beta(E_{c4}-E_c^2),\end{aligned} \tag{42}$$

$$\begin{aligned}\mathrm{Var}[X_2|b_l=+1]&=E[X_2^2|b_l=+1]-E^2[X_2|b_l=+1]\\&=4E^2\beta E_c^2,\end{aligned} \tag{43}$$

$$\begin{aligned}\mathrm{Var}[Y_2|b_l=+1]&=E[Y_2^2|b_l=+1]-E^2[Y_2|b_l=+1]\\&=(A^2+B^2)\beta N_0E_c,\end{aligned} \tag{44}$$

$$\begin{aligned}\mathrm{Var}[Z_2|b_l=+1]&=E[Z_2^2|b_l=+1]-E^2[Z_2|b_l=+1]\\&=\lambda^2\beta\frac{N_0^2}{4}.\end{aligned} \tag{45}$$

Due to the statistical independence between the components, i.e. W_1, X_1, Y_1, Z_1 and W_2, X_2, Y_2, Z_2, the mean value and variance of the decision variables, $s_l^{(1)}$ and $s_l^{(2)}$, are, respectively, determined as

$$\begin{aligned}E[s_l^{(1)}|b_l=+1]&=E[W_1|b_l=+1]+E[X_1|b_l=+1]\\&\quad+E[Y_1|b_l=+1]+E[Z_1|b_l=+1]\\&=E[W_1|b_l=+1],\end{aligned} \tag{46}$$

$$\begin{aligned}\mathrm{Var}[s_l^{(1)}|b_l=+1]&=\mathrm{Var}[W_1|b_l=+1]+\mathrm{Var}[X_1|b_l=+1]\\&\quad+\mathrm{Var}[Y_1|b_l=+1]+\mathrm{Var}[Z_1|b_l=+1].\end{aligned} \tag{47}$$

and

$$\begin{aligned}E[s_l^{(2)}|b_l=+1]&=E[W_2|b_l=+1]+E[X_2|b_l=+1]\\&\quad+E[Y_2|b_l=+1]+E[Z_2|b_l=+1]\\&=E[W_2|b_l=+1],\end{aligned} \tag{48}$$

$$\begin{aligned}\mathrm{Var}[s_l^{(2)}|b_l=+1]&=\mathrm{Var}[W_2|b_l=+1]+\mathrm{Var}[X_2|b_l=+1]\\&\quad+\mathrm{Var}[Y_2|b_l=+1]+\mathrm{Var}[Z_2|b_l=+1].\end{aligned} \tag{49}$$

Second, the case of a '−1' bit transmitted is considered. Similarly, we have

$$E[s_l^{(1)}|b_l=-1]=-E[s_l^{(1)}|b_l=+1], \tag{50}$$

$$\mathrm{Var}[s_l^{(1)}|b_l=-1]=\mathrm{Var}[s_l^{(1)}|b_l=+1], \tag{51}$$

and

$$E[s_l^{(2)}|b_l=-1]=-E[s_l^{(2)}|b_l=+1], \tag{52}$$

$$\mathrm{Var}[s_l^{(2)}|b_l=-1]=\mathrm{Var}[s_l^{(2)}|b_l=+1]. \tag{53}$$

Assuming that each bit, either '+1' or '−1', appears at the output of the data source with a probability of 1/2. Based on the obtained results above, the statical BER expressions for the SDS and DSS receivers can be, respectively, derived by the Gaussian

approximation as follows

$$\begin{aligned}\mathrm{BER}_{\mathrm{SDS}} &= \frac{1}{2}\Pr\left(s_l^{(1)} \le 0 | b_l = +1\right) + \frac{1}{2}\Pr\left(s_l^{(1)} > 0 | b_l = -1\right) \\ &= Q\left(\frac{\mathrm{Var}[s_l^{(1)} | b_l = +1]}{E^2[s_l^{(1)} | b_l = +1]}\right)^{-(1/2)} \\ &= Q\left(\frac{(A^4 + B^4)\left((E_{c4}/E_c^2) - 1\right) + 4A^2B^2}{\beta(A^2 + B^2)^2}\right. \\ &\quad + \frac{2}{(A^2 + B^2/\lambda^2)(E_\mathrm{b}/N_0)} \\ &\quad \left. + \frac{\beta}{\left((A^2 + B^2/\lambda^2)(E_\mathrm{b}/N_0)\right)^2}\right)^{-(1/2)}, \end{aligned} \tag{54}$$

and

$$\begin{aligned}\mathrm{BER}_{\mathrm{DSS}} &= \frac{1}{2}\Pr\left(s_l^{(2)} \le 0 | b_l = +1\right) + \frac{1}{2}\Pr\left(s_l^{(2)} > 0 | b_l = -1\right) \\ &= Q\left(\frac{\mathrm{Var}[s_l^{(2)} | b_l = +1]}{E^2[s_l^{(2)} | b_l = +1]}\right)^{-(1/2)} \\ &= Q\left(\frac{(C^2 + D^2)((E_{c4}/E_c^2) - 1) + 4E^2}{\beta(C + D)^2}\right. \\ &\quad + \frac{\left(2(A^2 + B^2)/(C + D)\lambda\right)}{(C + D/\lambda)(E_\mathrm{b}/N_0)} \\ &\quad \left. + \frac{\beta}{\left((C + D/\lambda)(E_\mathrm{b}/N_0)\right)^2}\right)^{-(1/2)}, \end{aligned} \tag{55}$$

where the function $Q(\cdot)$ is defined by

$$Q(\varepsilon) = \frac{1}{\sqrt{2\pi}}\int_\varepsilon^\infty \exp\left(y^2/2\right) \mathrm{d}y,$$

and $E_\mathrm{b} = 2\beta E_c$ is average bit energy.

In the studied channel, since the fading coefficients vary randomly according to the Rayleigh distribution, the elements within the brackets in (54) and (55), respectively, denoted by

$$\phi_{\mathrm{SDS}} = \frac{(A^4 + B^4)\left((E_{c4}/E_c^2) - 1\right) + 4A^2B^2}{\beta(A^2 + B^2)^2},$$

$$\gamma_{\mathrm{SDS}} = \frac{A^2 + B^2}{\lambda^2}\frac{E_\mathrm{b}}{N_0},$$

and

$$\phi_{\mathrm{DSS}} = \frac{(C^2 + D^2)((E_{c4}/E_c^2) - 1) + 4E^2}{\beta(C + D)^2},$$

$$\psi_{\mathrm{DSS}} = \frac{2(A^2 + B^2)}{(C + D)\lambda}, \quad \gamma_{\mathrm{DSS}} = \frac{C + D}{\lambda}\frac{E_b}{N_0}$$

also randomly vary in the communication process. Here, the elements, i.e. γ_{SDS} and γ_{DSS}, are considered as the main elements because they fully depend on the bit energy E_b and all parameters of the channel, i.e. L, α_j, τ_j, N_0. To simplify our analysis, the elements, ϕ_{SDS} and ϕ_{DSS}, ψ_{DSS} are considered as constants which are, respectively, equal to

$$\overline{\phi}_{\mathrm{SDS}} = \frac{(\overline{A}^4 + \overline{B}^4)\left((E_{c4}/E_c^2) - 1\right) + 4\overline{A}^2\overline{B}^2}{\beta(\overline{A}^2 + \overline{B}^2)^2},$$

and

$$\overline{\phi}_{\mathrm{DSS}} = \frac{(\overline{C}^2 + \overline{D}^2)((E_{c4}/E_c^2) - 1) + 4E^2}{\beta(\overline{C} + \overline{D})^2},$$

$$\overline{\psi}_{\mathrm{DSS}} = \frac{2(\overline{A}^2 + \overline{B}^2)}{(\overline{C} + \overline{D})\lambda}.$$

The constants, i.e. $\overline{A}$, $\overline{B}$, $\overline{C}$, $\overline{D}$, $\overline{E}$ are respectively obtained by replacing the variable coefficients α_j in A, B, C, D, E by their mean values, i.e. $\overline{\alpha}_j = \sigma_j\sqrt{\pi/2}$.

The statistical BER expressions in (54) and (55) are approximated by

$$\mathrm{BER}_{\mathrm{SDS}} \simeq Q\left(\overline{\phi}_{\mathrm{SDS}} + \frac{2}{\gamma_{\mathrm{SDS}}} + \frac{\beta}{\gamma_{\mathrm{SDS}}^2}\right)^{-(1/2)}, \tag{56}$$

and

$$\mathrm{BER}_{\mathrm{DSS}} \simeq Q\left(\overline{\phi}_{\mathrm{DSS}} + \frac{\overline{\psi}_{\mathrm{DSS}}}{\gamma_{\mathrm{DSS}}} + \frac{\beta}{\gamma_{\mathrm{DSS}}^2}\right)^{-(1/2)}. \tag{57}$$

On the basic of (56) and (57), the dynamical BER expressions reflecting the variation of fading coefficients corresponding to two proposed receivers are obtained as follows

$$\begin{aligned}\mathrm{BER}(\gamma_{\mathrm{SDS}})_{\mathrm{SDS}} &\simeq \int_0^\infty Q\left(\overline{\phi}_{\mathrm{SDS}} + \frac{2}{\gamma_{\mathrm{SDS}}} + \frac{\beta}{\gamma_{\mathrm{SDS}}^2}\right)^{-(1/2)} \\ &\quad \times f(\gamma_{\mathrm{SDS}})\,\mathrm{d}\gamma_{\mathrm{SDS}}, \end{aligned} \tag{58}$$

and

$$\begin{aligned}\mathrm{BER}(\gamma_{\mathrm{DSS}})_{\mathrm{DSS}} &\simeq \int_0^\infty Q\left(\overline{\phi}_{\mathrm{DSS}} + \frac{\overline{\psi}_{\mathrm{DSS}}}{\gamma_{\mathrm{DSS}}} + \frac{\beta}{\gamma_{\mathrm{DSS}}^2}\right)^{-(1/2)} \\ &\quad \times f(\gamma_{\mathrm{DSS}})\,\mathrm{d}\gamma_{\mathrm{DSS}}, \end{aligned} \tag{59}$$

with $f(\gamma_{\mathrm{SDS}})$ and $f(\gamma_{\mathrm{DSS}})$ being the probability density functions (PDF) of the elements γ_{SDS} and γ_{SDS}, respectively.

3.2 Performance in special cases of studied channel

In this subsection, we consider the performances of two proposed receivers in two special cases of the studied channel, i.e. AWGN channel and one-path Rayleigh fading channel. In the first case, an AWGN channel is equivalent to our channel in the case of $L = 1$ and $\alpha_1 = 1$. The values of parameters and elements are obtained as follows: $\lambda_1 = 0$, $\lambda_2 = \lambda$, $A = C = \lambda$, $B = D = E = 0$, $\overline{\phi}_{\mathrm{SDS}} = \overline{\phi}_{\mathrm{DSS}} = \left((E_{c4}/E_c^2) - 1\right)/\beta \simeq 0$, $\overline{\psi}_{\mathrm{DSS}} = 2$, and $\gamma_{\mathrm{SDS}} = \gamma_{\mathrm{DSS}} = E_\mathrm{b}/N_0$. The dynamical BER expressions in (58) and (59) become

$$\begin{aligned}\mathrm{BER}_{\mathrm{SDS}}\left(\frac{E_\mathrm{b}}{N_0}\right) &= \mathrm{BER}_{\mathrm{DSS}}\left(\frac{E_\mathrm{b}}{N_0}\right) \\ &\simeq Q\left(\frac{2}{(E_\mathrm{b}/N_0)} + \frac{\beta}{(E_\mathrm{b}/N_0)^2}\right)^{-(1/2)}. \end{aligned} \tag{60}$$

These BER results are exactly the same as that of the conventional DCSK system presented in [22, 23]. For the second case, one-path Rayleigh fading channel has been used for performance investigation of the conventional DCSK system in [24]. This channel is equivalent to our channel in the case of $L = 1$ and $\alpha_1 > 0$. Under this condition, we obtain the following values: $\lambda_1 = 0$, $\lambda_2 = \lambda$, $A = \lambda\alpha_1$, $C = \lambda\alpha_1^2$, $B = D = E = 0$, $\overline{\phi}_{\mathrm{SDS}} = \overline{\phi}_{\mathrm{DSS}} = \left((E_{c4}/E_c^2) - 1\right)/\beta \simeq 0$, $\overline{\psi}_{\mathrm{DSS}} = 2$,

and $\gamma_{SDS} = \gamma_{DSS} = \alpha_1^2 E_b/N_0$. The PDFs are determined by

$$f(\gamma_{SDS}) = f(\gamma_{DSS}) = \frac{1}{2\sigma_1^2(E_b/N_0)} e^{-(\alpha_1^2/2\sigma_1^2)}$$

The dynamical BER expressions become as follows

$$\begin{aligned} BER_{SDS}\left(\alpha_1^2\frac{E_b}{N_0}\right) &\simeq BER_{DSS}\left(\alpha_1^2\frac{E_b}{N_0}\right) \\ &\simeq \int_0^\infty Q\left(\frac{2}{\alpha_1^2(E_b/N_0)} + \frac{\beta}{(\alpha_1^2(E_b/N_0))^2}\right)^{-(1/2)} \\ &\quad \frac{1}{2\sigma_1^2(E_b/N_0)} e^{-(\alpha_1^2/2\sigma_1^2)} d\left(\alpha_1^2\frac{E_b}{N_0}\right). \end{aligned} \tag{61}$$

This result is also the BER expression obtained in [24]. We can find that the obtained results in (60) and (61) totally agree with the results in the previous studies in [22–24], respectively. It means that the performances under AWGN and one-path Rayleigh fading channels of the SDS and DSS receivers are the same as those of the conventional receiver. However in our study, the channel under investigation is the frequency non-selective Rayleigh fading channel which is generalised with the number of paths $L \geq 2$, Therefore, the more number of secondary paths L, the more complicated, if not impossible, the theoretical determination of the $f(H)$ is. For this reason, another simpler approach to estimate the PDFs and performances using numerical integration is presented in the next subsection.

3.3 Numerical integration

In this approach, the numerical computation method proposed in [45] is used to determine histograms of value distribution of γ_{SDS} and γ_{DSS} instead of theoretically determining their PDFs. The sample values of γ_{SDS} and γ_{DSS} are first computed and then used to build the histogram of value distribution. With the assumption that the values of γ_{SDS} and γ_{DSS} are the outputs of stationary random processes [46], the obtained histograms can be considered as a good estimation of the PDFs. Based on the BER expressions theoretically obtained in (58) and (59) as well as the distribution histograms obtained by the computation, the BER performances of two proposed receivers can be respectively calculated by the following numerical integrations

$$\begin{aligned} &BER_{SDS}(\gamma_{SDS}) \\ &\simeq \sum_{m=1}^{N} Q\left(\overline{\phi}_{SDS} + \frac{2}{\gamma_{SDS,m}} + \frac{\beta}{\gamma_{SDS,m}^2}\right)^{-(1/2)} \times P(\gamma_{SDS,m}), \end{aligned} \tag{62}$$

and

$$\begin{aligned} &BER_{DSS}(\gamma_{DSS}) \\ &\simeq \sum_{m=1}^{N} Q\left(\overline{\phi}_{DSS,m} + \frac{\overline{\psi}_{DSS,m}}{\gamma_{DSS,m}} + \frac{\beta}{\gamma_{DSS,m}^2}\right)^{-(1/2)} \times P(\gamma_{DSS,m}), \end{aligned} \tag{63}$$

where N is the number classes of the histogram and $P(\gamma_{DSS,m})$ is the probability of having the energy in intervals centred on $\gamma_{DSS,m}$.

4 Simulation results and comparison

In this section, the performances of two receivers obtained by the analysis according to (62), (63) and the corresponding numerical simulations are displayed in the same graphs for the comparison. The figures display the BER performance with respect to the typical parameters, i.e. the ratio E_b/N_0, spreading factor 2β, and number of samples per chip λ, when the number of paths L gradually increases from 2 to 5. The chaotic map used for generating the chaotic sequence is the Chebyshev polynomial function of order 2 [47] given by

$$x_k = f(x_{k-1}) = 2x_{k-1}^2 - 1, \tag{64}$$

with the invariant PDF of x, denoted by $\rho(x)$ being

$$\rho(x) = \begin{cases} \dfrac{1}{\pi\sqrt{1-x^2}} & |x| < 1, \\ 0 & \text{otherwise.} \end{cases} \tag{65}$$

The values of E_c and E_{c4} are determined by

$$E_c = E\left[x_{k,l}^{(i)\,2}\right] = \int_{-\infty}^{\infty} x^2\rho(x)\,dx = \int_{-1}^{1} x^2 \frac{1}{\pi\sqrt{1-x^2}}\,dx = \frac{1}{2}. \tag{66}$$

$$E_{c4} = E\left[x_{k,l}^{(i)\,4}\right] = \int_{-\infty}^{\infty} x^4\rho(x)\,dx = \int_{-1}^{1} x^4 \frac{1}{\pi\sqrt{1-x^2}}\,dx = \frac{3}{8}. \tag{67}$$

The parameters of the channel are set as follows: $\sigma_1 = 0.7$ for the primary path; $\sigma_2 = 0.6$, $\tau_2 = 5$, $\sigma_3 = 0.5$, $\tau_3 = 10$, $\sigma_4 = 0.4$, $\tau_4 = 15$, and $\sigma_5 = 0.3$, $\tau_5 = 20$, for the secondary paths.

Fig. 3 shows the histograms of value distribution of γ_{SDS} and γ_{DSS} obtained by the numerical computations for the case of $E_b/N_0 = 10$ dB and $\lambda = 30$. Each histogram was plotted by means of $N = 1000$ classes which are calculated statistically from 100,000 samples. It clearly appears that the increment of L leads to the changes of value distribution, specifically, the average values and variation ranges of $\gamma_{SDS,m}$ and $\gamma_{DSS,m}$ increases. In addition, with the same value of L, the average value and variation range of $\gamma_{DSS,m}$ is always higher than those of $\gamma_{SDS,m}$. Due to the property of Q function, we can find from (62) and (63) that these changes will make the BERs reduce, where the reduced amount of the DSS receiver is greater than that of the SDS one.

In Fig. 4, we study the effect of the ratio E_b/N_0 and number of paths L on the performance of the receivers in the case of $\lambda = 30$ and $\beta = 32$. The BER performances obtained in (60) and (61) for the special cases of the channel with $L = 1$ are also plotted. It can be seen that there is a good match between the analysis and

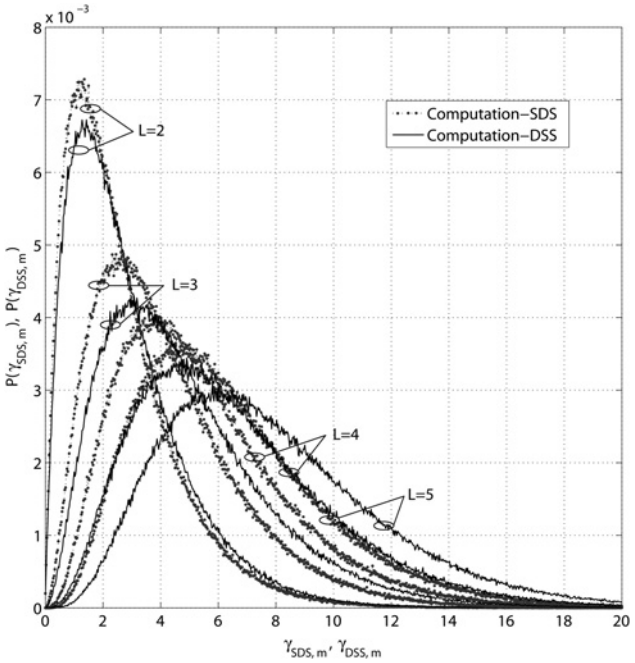

Fig. 3 *Histograms of the value distribution of the elements, γ_{SDS} and γ_{DSS}, in the case of $E_b/N_0 = 10$ dB and $\lambda = 30$*

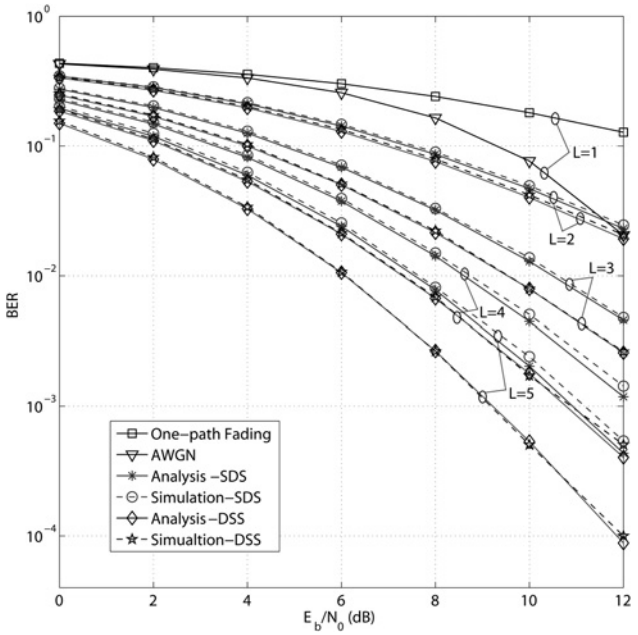

Fig. 4 *BER values against the ratio E_b/N_0 in the case of $\beta = 32$ and $\lambda = 30$*

simulation performances. We can find interesting results, i.e. the performance of the receivers is significantly improved when the number of paths increases, where the performance of the DSS receiver gets better than that of the SDS with the higher value of L. For example at the same $E_b/N_0 = 10$ dB, the BER values of the SDS and DSS receiver corresponding to $L = 1, 2, 3, 4, 5$ are $1.9 \cdot 10^{-1}$, $5.1 \cdot 10^{-2}$, $1.2 \cdot 10^{-2}$, $5.2 \cdot 10^{-3}$, $2.3 \cdot 10^{-3}$; and $1.9 \cdot 10^{-1}$, $4.2 \cdot 10^{-2}$, $7.9 \cdot 10^{-3}$, $1.4 \cdot 10^{-3}$, $5.3 \cdot 10^{-4}$, respectively.

The effect of the value of the spreading factor on the BER performance in the case of $E_b/N_0 = 10$ dB and $\lambda = 30$ is shown in Fig. 5. We can observe that in the value range from 20 to 98, the value increment of β and corresponding BERs is directly proportional to each other. For example with the case of $L = 3$, the BER values for the SDS and DSS receiver increase, respectively, from $1.1 \cdot 10^{-2}$ and $5.1 \cdot 10^{-2}$ to $2.9 \cdot 10^{-2}$ and $1.9 \cdot 10^{-2}$

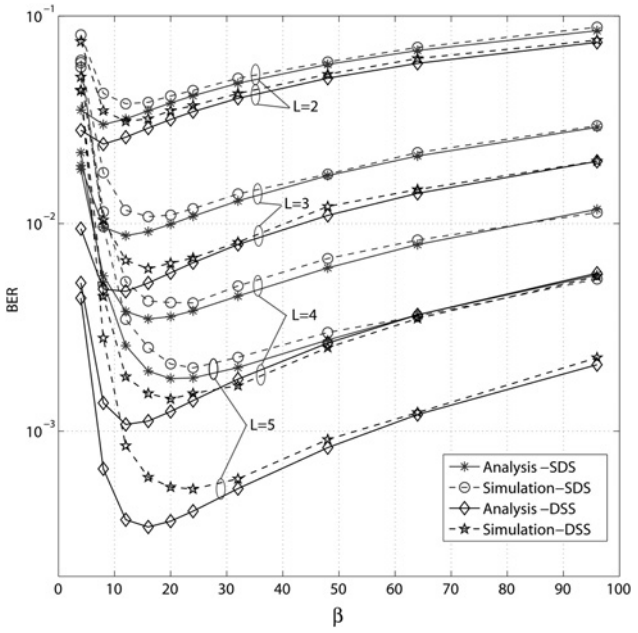

Fig. 5 *BER values against the spreading factor 2β in the case of $E_b/N_0 = 10$ and $\lambda = 30$*

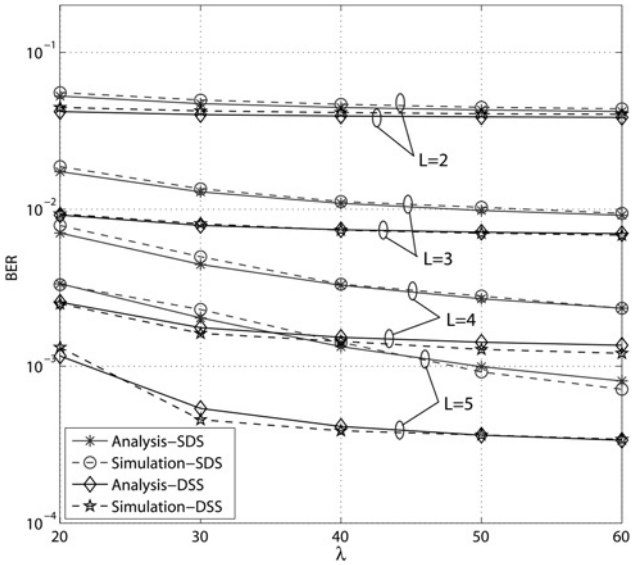

Fig. 6 *BER values against the number of samples per chip λ in the case of $E_b/N_0 = 10$ and $\beta = 30$*

corresponding to β changing from 20 to 98. In contrast, in the value range from 4 to 20, the increment of β makes the BERs reduce. In particular, the minimum values of BER are obtained with the value of β within 10 and 20. It means that the good performance is obtained at low values of spreading factor, or in other words, our proposed receivers can perform well even with a moderate bandwidth. Generally, the simulation results exactly agree with the analysis ones except for the range of $\beta \leq 20$. The differences become more pronounced at higher values of L. There are two causes for these differences. First, our assumption in Section 3.1, i.e. the correlation values of the independent variables are approximately equal to zero, is no longer satisfied with low spreading factor. Second, the elements, ϕ_{SDS} and ϕ_{DSS}, ψ_{DSS}, in (54) and (55) are approximated by the constants, $\overline{\phi}_{SDS}$ and $\overline{\phi}_{DSS}$, $\overline{\psi}_{DSS}$, in (56) and (57), respectively. Note that these assumption and approximation aim to simplify our BER analysis but simultaneously they also create the differences.

Fig. 6 shows the dependence of BER values upon the number of samples per chip λ in the case of $E_b/N_0 = 10$ and $\beta = 32$. It clearly appears that the performance of the receivers is enhanced when the value of λ is increased. For example with the case of $L = 5$, the BER values of the SDS and DSS receivers reduce, respectively,

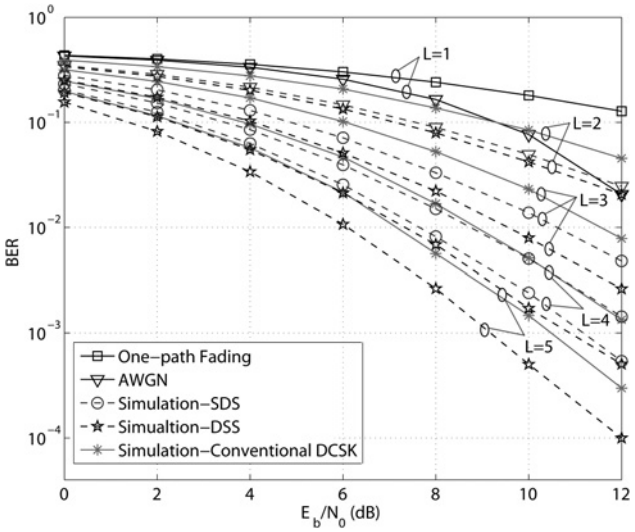

Fig. 7 *BER performance comparison in the case of $\beta = 32$ and $\lambda = 30$*

IET Commun., 2016, Vol. 10, Iss. 11, pp. 1263–1272

Table 1 Number of funtional blocks used in transmitter (Tx) and receiver (Rx) of different DCSK systems

Used blocks	Systems									
	Conventional DCSK		FM-DCSK		MIMO DCSK-CD		MC-DCSK		Proposed DCSK	
	Tx	Rx	Tx	Rx	Tx	Rx	Tx	Rx	Tx	Rx
chaos generator	1	0	1	0	1	0	1	0	1	0
delay block	1	1	1	1	N	N	0	0	1	1
signal multiplier	1	1	1	1	$N-1$	$2N+2$	$2M-1$	M	1	1
switching block	1	0	1	0	1	0	0	0	1	0
sum block	0	1	0	1	0	2	1	0	0	2
decision circuit	0	1	0	1	0	1	0	1	0	1
FM modulator	0	0	1	0	0	0	0	0	0	0
filter	0	0	0	1	0	0	0	M	0	0
S/P or P/S converter	0	0	0	0	0	0	1	1	0	0
store matrix	0	0	0	0	0	0	0	2	0	0
matrix multiplier	0	0	0	0	0	0	0	1	0	0
over-sampling block	0	0	0	0	0	0	0	0	0	1
Walsh-code generator	0	0	0	0	1	1	0	0	0	0

from $3.1 \cdot 10^{-3}$ and $1.2 \cdot 10^{-3}$ to $7.5 \cdot 10^{-4}$ and $3.3 \cdot 10^{-4}$ corresponding to the value of λ increasing from 20 to 60. As can be clearly seen from this figure that the analysis agreed very well with the simulations.

The comparison of BER performance between the SDS, DSS and conventional DCSK receivers is displayed in Fig. 7. It clearly appears that the performance of the conventional scheme is the same as that of the proposed ones in the case of $L = 1$. In particular, the SDS scheme performs better than the conventional one in the cases of $L = 2, 3$, nearly the same when $L = 4$, yet worse in the case of $L = 5$. However, in all the cases of $L = 2, 3, 4, 5$, the performance of DSS scheme is always better than that of the SDS and conventional ones. For example at the same $E_b/N_0 = 10$ dB, BER values of the conventional, SDS, and DSS receivers corresponding to $L = 2, 3, 4, 5$ are $8.4 \cdot 10^{-2}$, $2.3 \cdot 10^{-2}$, $5.1 \cdot 10^{-3}$, $1.5 \cdot 10^{-3}$; $5.1 \cdot 10^{-2}$, $1.2 \cdot 10^{-2}$, $5.2 \cdot 10^{-3}$, $2.3 \cdot 10^{-3}$; and $4.2 \cdot 10^{-2}$, $7.9 \cdot 10^{-3}$, $1.4 \cdot 10^{-3}$, $5.3 \cdot 10^{-4}$, respectively.

5 Discussion on implementation complexity

This section presents our discussion on the implementation complexity of the proposed DSS receiver. Since the DSS receiver performs the demodulation to recover the data based on the discrete-sampling process, the hardware implementation can be carried out with the use of high-speed programmable CHIPs such as FPGA, DPS, or Microcontroller. All blocks in the proposed schemes can be implemented by available or created modules on the same CHIP. For example, the sampler at the input can be done by an ADC module, in which the received signal is sampled and converted into binary values restored in registers. The delay block can be realised by a counter or a timer. The multiplication, sum, and threshold comparison of discrete samples are then done by corresponding calculations with respect to the binary values on the registers. In addition, with the simple architectures, the receivers can achieve low power consumption, low cost and small size. Table 1 shows the number of functional blocks used in the transmitter and receiver of different DCSK systems. We can see that the conventional DCSK system proposed in [25] has the simplest architecture, where the transmitter consists of a chaotic sequence generator, a delay block, a multiplier, and a switching block, while the receiver is composed by a delay block, a multiplier, a sum block, and a decision circuit. In the FM-DCSK system [29], beside the above components, a FM modulator and a channel filter are added to the inputs of the transmitter and receiver, respectively. The architecture of MC-DCSK [34] and MIMO DCSK-CD [39] systems is much more complicated than that of the original one. The MC-DCSK transmitter uses a chaos generator, $(2M-1)$ multipliers with M being number of subcarriers, a sum block, and a serial/parallel (S/P) converter, while its receiver includes M multipliers, M matched filters, two store matrices and a matrix multiplier, a P/S converter, and a decision circuit. With respect to the MIMO DCSK-CD system, multiple-access is performed by adopting the orthogonal Walsh code sequences, in which the relay and destination both employ multiple antennas to strengthen the robustness against signal fading in a wireless network. In particular, the MIMO DCSK-CD receiver is based on the generalised maximum likelihood detector, which consists of N delay blocks and $(2N+2)$ multipliers with N being the number of users, two sum blocks, a Walsh-code generator, and a decision circuit. For the sake of simple architecture, the oversampling-based DCSK system under our study uses the same transmitter as the original one. Basically, the proposed scheme of DSS receiver is based on that of the conventional one, where a oversampler and a sum block are, respectively, added to the input and output of the correlator. It can be found from the above description that the architecture of our DCSK system with DSS receiver is more complicated than that of the conventional one, but simpler than that of the FM-DCSK system and much simpler than those of the MC-DCSK and MIMO DCSK-CD systems.

6 Conclusion

Two direct sampling DCSK receivers operating based on the same hardware platform with different structures, i.e. SDS and DSS, have been proposed for communication at physical layer under frequency non-selective fading channels. The mathematical modelling in discrete-time domain of the DCSK system under study, which consists of the conventional transmitter, the generalised non-selective Rayleigh fading with multiple transmission paths, and the proposed receivers were presented. The BER performance was analysed in detail by means of the combined method of theoretical derivation and numerical integration. The simulated performances were shown to verify the corresponding analysed ones. It can be found from the obtained results that both receivers can perform well under the studied channel and their performance gets increasingly better when the number of paths gradually increases. It means that the receivers can exploit the non-selective-fading characteristic of multipath channels to improve their performance. In particular, our comparison showed that under the same condition, the performance of the DSS receiver is always better than that of the SDS and conventional ones, and this performance difference gets larger with a higher number of paths. The aforementioned features make the DSS receiver along with the conventional transmitter be a promising and robust solution in the design of secure physical layer with low complexity, low cost, low power consumption, and small size for communications between nodes in LR-WPANs. The hardware implementation and performance measurement of the DSS receiver are also our future work.

7 Acknowledgment

This work was supported in part by the Newton Institutional Link under Grant ID 172719890.

8 References

1 Prasad, R., Munoz, L.: 'WLANs and WPANs towards 4G wireless' (Artech House, 2003)
2 Zheng, J., Lee, M.J., Anshel, M.: 'Toward secure low rate wireless personal area networks', *IEEE Trans. Mob. Comput.*, 2006, **5**, (10), pp. 1361–1373
3 IEEE 802.11: Wireless LANs, http://standards.ieee.org, 2013
4 Zheng, J., Lee, M.J.: 'Will IEEE 802.15.4 make ubiquitous networking a reality?-A discussion on a potential low power, low bit rate standard', *IEEE Commun. Mag.*, 2004, **42**, (6), pp. 140–146
5 Bisdikian, C.: 'An overview of the Bluetooth wireless technology', *IEEE Commun. Mag.*, 2001, **39**, (12), pp. 86–94
6 Wheeler, A.: 'Commercial applications of wireless sensor networks using ZigBee', *IEEE Commun. Mag.*, 2007, **45**, (4), pp. 70–77
7 Lau, F.C.M., Tse, C.K.: 'Chaos-based digital communication systems: operating principles, analysis methods, and performance evaluation' (Springer, 2003)
8 Berber, S., Chen, N.: 'Physical layer design in wireless sensor networks for fading mitigation', *J. Sens. Actuator Netw.*, 2013, **2**, (3), pp. 614–630
9 Talabani, A.A., Nallanathan, A., Nguyen, H.X.: 'Enhancing physical layer security of cognitive radio transceiver via chaotic OFDM'. 2015 IEEE Int. Conf. on Communication (ICC), London, June 2015, pp. 6421–6426
10 Heidari-Bateni, G., McGillem, C.D.: 'A chaotic direct-sequence spread-spectrum communication system', *IEEE Trans. Commun.*, 1994, **42**, pp. 1524–1527
11 Tam, W., Lau, F., Tse, C., *et al.*: 'Exact analytical bit error rates for multiple access chaos-based communication systems', *IEEE Trans. Circuits Syst. II*, 2004, **51**, (9), pp. 473–481
12 Kaddoum, G., Roviras, D., Charge, P., *et al.*: 'Robust synchronization for asynchronous multi-user chaos-based DS-CDMA', *Signal Process.*, 2009, **89**, (5), pp. 807–818
13 Quyen, N.X., Yem, V.V., Hoang, T.M.: 'A chaos-based secure direct-sequence/spread-spectrum communication system', *Abs. Appl. Anal.*, **2013**, p. 11, Article ID 764341, doi: 10.1155/2013/764341
14 Berber, S.M.: 'Probability of error derivatives for binary and chaos-based CDMA systems in wide-band channels', *IEEE Trans. Wirel. Commun.*, 2014, **13**, (10), pp. 5596–5606
15 Quyen, N.X., Cong, L.V., Long, N.H., *et al.*: 'An OFDM-based chaotic DSSS communication system with MPSK modulation'. Proc. Int. Conf. Communications and Electronics (ICCE'14), Danang, Vietnam, July 2014, pp. 106–111
16 Quyen, N.X., Yem, V.V., Duong, T.Q.: 'Design and analysis of a spread-spectrum communication system with chaos-based variation of both phase-coded carrier and spreading factor', *IET Commun.*, 2015, **9**, (12), pp. 1466–1473
17 Kolumban, G., Vizvari, B., Schwarz, W., *et al.*: 'Differential chaos shift keying: a robust code for chaos communication'. Proc. 4th Int. Workshop on Nonlinear Dynamics Electronic Systems, 1996, pp. 87–92
18 Lau, F.C.M., Yip, M.M., Tse, C.K., *et al.*: 'A multiple-access technique for differential chaos shift keying', *IEEE Trans. Circuits Syst.*, 2002, **49**, pp. 96–104
19 Kaddoum, G., Olivain, J., Samson, G. B., Giard, P., Gagnon, F.: 'Implementation of a differential chaos shift keying communication system in GNU radio'. Proc. 2012 Int. Symp. on Wireless Communication Systems, Paris-France, 2012, pp. 934–938
20 Mandal, S., Banerjee, S.: 'Analysis and CMOS implementation of a chaos-based communication system', *IEEE Trans., Circuits Syst. I-Reg. Pap.*, 2004, **51**, (9), pp. 1708–1722
21 Delgado-Restituto, M., Acosta, A.J., Rodriguez-Vazquez, A.: 'A mixed-signal integrated circuit for FM-DCSK modulation', *IEEE J. Solid-State Circuits*, 2005, **40**, (7), pp. 1460–1471
22 Sushchik, M., Tsimring, L.S., Volkovskii, A.R.: 'Performance analysis of correlation-based communication schemes utilizing chaos', *IEEE Trans. Circuits Syst.*, 2000, **47**, pp. 1684–1691
23 Kaddoum, G., Charge, P., Roviras, D., *et al.*: 'Performance analysis of differential chaos shift keying over an AWGN channel'. ACTEA 2009, Lebanon, 2009, pp. 255–358
24 Zhou, Z., Wang, J., Ye, Y.: 'Exact BER analysis of differential chaos shift keying communication system in fading channel', *Trans. Wirel. Pers. Commun.*, 2010, **53**, pp. 299–310
25 Xia, Y., Tse, C.K., Lau, F.C.M.: 'Performance of differential chaos-shift-keying digital communication systems over a multipath fading channel with delay spread', *IEEE Trans. Circuits Syst. II, Express Briefs*, 2004, **51**, pp. 680–684
26 Xia, Y., Tse, C.K., Fau, F.C.M., *et al.*: 'Performance of frequency-modulated differential chaos-shift-keying communication system over multipath fading channels with delay spread', *Int. J. Bifur. Chaos*, 2005, **15**, pp. 4027–4033
27 Zhou, Z., Zhou, T., Wang, J.: 'Performance of multiple access DCSK communication over multipath fading channel with delay spread', *Circuits, Syst. Signal Process.*, 2008, **27**, pp. 507–518
28 Chong, C.C., Yong, S.K.: 'UWB direct chaotic communication technology for low-Rate WPAN applications', *IEEE Trans. Veh. Technol.*, 2008, **57**, (3), pp. 1527–1536
29 Kolumban, G., Kis, G., Jako, Z., *et al.*: 'FM-DCSK: A robust modulation scheme for chaotic communications', *IEICE Trans. Fund. Electron. Commun. Comput. Sci.*, 1998, **E81-A**, (9), pp. 1798–1802
30 Lau, F.C.M., Cheong, K.Y., Tse, C.K.: 'Permutation-based DCSK and multiple access DCSK systems', *IEEE Trans. Circuits Syst. I, Fundam. Theory Appl.*, 2003, **50**, (6), pp. 733–742
31 Yang, H., Jiang, G.P.: 'Reference-modulated DCSK: a novel chaotic communication scheme', *IEEE Trans. Circuits Syst. II*, 2013, **60**, (4), pp. 232–236
32 Kaddoum, G., Gagnon, F.: 'Design of a high-data-rate differential chaos-shift keying system', *IEEE Trans. Circuits Syst. II Express Briefs*, 2012, **57**, (9), pp. 448–452
33 Yang, H., Jiang, G.P.: 'High-efficiency differential-chaos-shift keying scheme for chaos-based noncoherent communication', *IEEE Trans. Circuits Syst. II Express Briefs*, 2012, **59**, (5), pp. 312–316
34 Kaddoum, G., Richardson, F.D., Gagnon, F.: 'Design and analysis of a multi-carrier differential chaos shift keying communication system', *IEEE Trans. Commun.*, 2013, **61**, (8), pp. 3281–3291
35 Fang, Y., Wang, L., Chen, P., *et al.*: 'Design and analysis of a DCSK-ARQ/CARQ system over multipath fading channels', *IEEE Trans. Circuits Syst. I: Reg. Papers*, 2015, **62**, (6), pp. 1637–1647
36 Kaddoum, G., Soujeri, E., Arcila, C., *et al.*: 'I-DCSK: An improved non-coherent communication system architecture', *IEEE Trans. Circuits Syst. II Express Briefs*, 2015, **62**, (9), pp. 901–905
37 Wang, L., Min, X., Chen, G.: 'Performance of SIMO FM-DCSK UWB system based on chaotic pulse cluster signals', *IEEE Trans. Circuits Syst. I*, 2011, **58**, (9), pp. 2259–2268
38 Wang, S., Wang, X.: 'M-DCSK-based chaotic communications in MIMO multipath channels with no channel state information', *IEEE Trans. Circuits Syst. II Express Briefs*, 2010, **57**, (12), pp. 1001–1005
39 Fang, Y., Xu, J., Wang, L., *et al.*: 'Performance of MIMO relay DCSK-CD systems over Nakagami fading channels', *IEEE Trans. Circuits Syst. I*, 2013, **60**, (3), pp. 757–767
40 Xu, W., Wang, L., Chen, G.: 'Performance of DCSK cooperative communication systems over multipath fading channels', *IEEE Trans. Circuits Syst. I*, 2011, **58**, (1), pp. 196–204
41 Gilbert, E.N.: 'Increased information rate by oversampling', *IEEE Trans. Inf. Theory*, 1993, **39**, (6), pp. 1973–1976
42 El-Khaldi, B., Rouvaen, J.M., Menhaj, A., *et al.*: 'Averaging and oversampling correlator receiver with input quantization', *Digital Signal Process.*, 2006, **16**, (2), pp. 120–136
43 Leeand, Y.S., Seo, B.S.: 'OFDM receivers using oversampling with rational sampling ratios', *IEEE Trans. Consum. Electron.*, 2009, **55**, (4), pp. 1765–1770
44 Arauz, J., Krishnamurthy, P., Labrador, M.A.: 'Discrete Rayleigh fading channel modeling', *Wirel. Commun. Mob. Comput.*, 2004, **4**, (4), pp. 413–425
45 Kaddoum, G., Charge, P., Roviras, D.: 'A generalized methodology for bit-error-rate prediction in correlation-based communication schemes using chaos', *IEEE Commun. Lett.*, 2009, **13**, pp. 567–569
46 Isabelle, S.H., Wornell, G.W.: 'Statistical analysis and spectral estimation techniques for one-dimensional chaotic signals', *IEEE Trans. Signal Process.*, 1997, **45**, pp. 1495–1497
47 Geisel, T., Fairen, V.: 'Statistical properties of chaos in Chebyshev maps', *Phys. Lett.*, 1984, **105A**, (6), pp. 263–266